Residual stress effects on fatigue life prediction using hardness measurements for butt-welded joints made of high strength steels

Xin, Haohui; Correia, José A.F.O.; Veljkovic, Milan; Berto, Filippo; Manuel, Lance

DOI
10.1016/j.ijfatigue.2021.106175

Publication date
2021

Document Version
Final published version

Published in
International Journal of Fatigue

International Journal of Fatigue 147 (2021) 106175

Contents lists available at ScienceDirect

International Journal of Fatigue

journal homepage: www.elsevier.com/locate/ijfatigue

Residual stress effects on fatigue life prediction using hardness measurements for butt-welded joints made of high strength steels

Haohui Xin [a,*], José A.F.O. Correia [b], Milan Veljkovic [c], Filippo Berto [d], Lance Manuel [e]

[a] Department of Civil Engineering, School of Human Settlements and Civil Engineering, Xi'an Jiaotong University, China
[b] INEGI & CONSTRUCT, Faculty of Engineering, University of Porto, Portugal
[c] Faculty of Civil Engineering and Geosciences, Delft University of Technology, Netherlands
[d] Department of Mechanical and Industrial Engineering, Norwegian University of Science and Technology (NTNU), Norway
[e] Department of Civil, Architectural and Environmental Engineering, The University of Texas at Austin, USA

ARTICLE INFO

Keywords:
Butt-welded plates
Hardness measurements
Residual stress effects
S-N curves

ABSTRACT

The fatigue resistance of welded connections made of high strength steel (HSS) is one of the most important topics for the application of HSS in the construction sector. One of the most challenging issues is how to predict the fatigue life of welded structures with complex geometry based on the test results from relatively simple coupon specimens. However, there are generally pre-existing residual stresses in the welded coupon specimens during fatigue tests, and these residual stresses vary greatly in welded structures with complex geometry. This increases the difficulty in predicting the fatigue behaviour of welded structures based on results at coupon scale. Hence, it is important to establish a relationship between the residual stress independent material characteristics and fatigue life. The fatigue behaviour of complex welded structures can be predicted by this residual stress independent material characteristics calibrated at the coupon level and simulated local residual stress distribution. In this paper, the residual stress-free characteristics, hardness, is employed to predict the fatigue life of butt-welded joints. Besides, the residual stress of V-shaped butt welds on a plate made of high strength steels are analysed by modelling of the welding process based on subsequent thermal analysis and mechanical stress analysis by implementing kill/birth strategies. The results show that it contributes to a better prediction compared with experimental results after considering the residual stress effects.

1. Introduction

High strength steel (HSS) could provide economical solutions for highly loaded slender members in long-span or high-rise structures [1-3]. Despite the benefits of increased yield strength, the fatigue resistance of steel structures especially welded connections, is one of the most important concerns [4]. Nowadays, the main methodology to determine the fatigue behaviour of the complex steel structures is through experimental observations [5]. The long test period and expensive costs are the main complaints of such larger fatigue tests. It is necessary to use computer-aided methods to complement large-scale fatigue tests. One of the most challenging issues is how to predict the fatigue life of welded structures with complex geometry based on test results from relatively simple coupon specimens.

Welding technology makes the connections of steel structures simple and convenient. However, local welding heat introduces an abrupt temperature increase, followed by subsequent cooling to room temperature. This process leads to defects, misalignments, and residual stresses because of the restrained shrinkage of the heated zone by the surrounded cooler zone. The residual stress will affect fatigue crack initiation and propagation at the welded joints [6-8]. Teng et al. [9,10] evaluated the residual stress effect on the fatigue lifetime of butt welded plates based on thermal elastic–plastic analysis and the strain-life method. Dong et al. [11] assessed the residual stress effect on fatigue crack initiation of fillet welds after ultrasonic impact treatment based on the local strain approach. Xin et al. [8] investigated residual stresses on fatigue crack initiation of butt-welded plates made of high strength steels. Results showed that residual stresses influence fatigue crack initiation position and the fatigue behaviour of butt-welded plates. A relatively simple engineering approach that neglects the phase transformation effects and that evaluates whether it is possible to predict the fatigue crack growth rate of welded joints based on the parent material

* Corresponding author.
E-mail address: xinhaohui@xjtu.edu.cn (H. Xin).

https://doi.org/10.1016/j.ijfatigue.2021.106175
Received 18 December 2020; Received in revised form 23 January 2021; Accepted 26 January 2021
Available online 5 February 2021

based on fatigue experiments has also been discussed by Xin [7]. Results showed that it is promising to predict fatigue crack growth rate parameters based on the parent material and residual stresses if fatigue experiments are unavailable due to cost and time limitations.

Residual stresses already exist in welded coupon specimens during fatigue tests, but these residual stresses change a lot in welded structures with complex geometry. This increases the difficulties in predicting the fatigue performance of welded structures or joints with complex geometry based on fatigue test results conducted at coupon scale. Hence, it is important to build a relationship between residual stress independent material characteristics and fatigue life.

A residual stress-free property, hardness, is a good alternative to predict the fatigue life of welded joints. Bandara et al. [12,13] proposed a full range of stress-life curves, that describe fatigue S-N curve variation from the first cycle (at ultimate tensile strength) up to 10^9 cycles (gigacycles) based on the ultimate tensile strength and Vickers hardness. Strzelecki & Tomaszewski [14] presented an analytical study on fatigue behaviour of materials and construction elements based on hardness measurements, where they employed a relationship between hardness and tensile strength, as well as a fatigue limit. Correia et al. [15] suggested a generalization of the Kohout-Vechet fatigue model, a full-range curve from quasi-static monotonic loading to long-term cyclic loading, for different local fatigue damage criteria based on stress, strain, and energy. Roessle and Fatemi [16] used hardness and elastic modulus to predict strain-controlled fatigue properties of the ASE steel series. Results showed that strain-fatigue life could be approximately predicted using hardness. Shamsaei and Fatemi [17] use hardness parameters to predict the fatigue performance of stainless steel exposed to a wide range of loading conditions. The results showed that the experimental fatigue life agreed well with predicted values based on hardness. The research studies discussed above focused mainly on the fatigue life prediction of the base material using hardness. Frankel et al. [18] proposed a model by fitting data on hardness versus residual stress that can be applied to estimate the residual stresses in metallic materials. The fatigue life prediction of butt-welded joints made of high strength steels, based on hardness measurements, residual stress effects and the hot-spot concept, is the main discussion of this paper.

Accordingly, the residual stress-free property, hardness, is employed to predict the fatigue life of butt-welded joints using a full range of S-N curves based on hardness values in this paper. Besides, the residual stress of HSS V-shaped butt welds joints is thoroughly analysed by modelling of the welding process based on subsequent thermal analysis and mechanical stress analysis by implementing kill/birth strategies. The residual stress effects on the fatigue life prediction of butt-welded joints made of HSS using hardness values and the hot-spot concept are discussed.

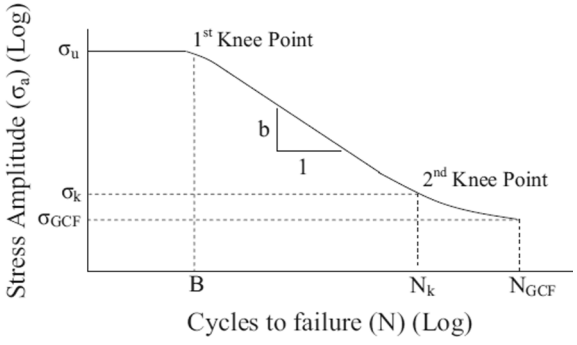

Fig. 1. Illustration of the full range S-N curve using hardness values [13].

2. Fatigue life prediction using hardness measurements

2.1. Full range S-N curves based on hardness measurements

A full range S-N relationship, see Fig. 1, including low cycle fatigue ($N \leq 10^4$), high cycle fatigue ($10^4 < N \leq 10^7$), and very high cycle fatigue ($N > 10^7$), is proposed by Bandara et al. [12,13], to predict the fatigue life of steels exposed to axial loading. The cycle-dependent fatigue strength is expressed in Eq. (1), and the related parameters could be predicted through Eqs. (2)–(7).

$$\sigma(N) = a(N+B)^b + c \tag{1}$$

$$B = \left(\frac{\sigma_u - c}{a}\right)^{1/b} \tag{2}$$

$$a = \frac{\sigma_{GCF} - \sigma_k}{N_{GCF}^b - N_k^b} \tag{3}$$

$$c = \frac{\sigma_{GCF} N_{GCF}^b - \sigma_k N_k^b}{N_{GCF}^b - N_k^b} \tag{4}$$

$$\sigma_u = 2\sigma_k = 3.34Hv \tag{5}$$

$$\sigma_{GCF} = \frac{\sigma_u^{1/3}}{1000}(H_v + 120)(155 - 7logN_{GCF}) \tag{6}$$

$$N_k = 10^{\left(\frac{0.155(Hv+120)\sigma_u^{1/3} - 0.5\sigma_u}{0.007(Hv+120)\sigma_u^{1/3}}\right)} \tag{7}$$

where the slope b is in the range of -0.12 to -0.21, and is suggested to be -0.20 in Ref. [13]. B is the number of cycles to failure at the 1st knee point.N_k is the number of cycles to failure at the 2nd knee point. N_{GCF} is the number of cycles to failure in the gigacycle region, assumed to be 1×10^9. σ_u is the ultimate tensile strength. H_v is the Vicker's hardness. σ_{GCF} is the fatigue strength in the gigacycle region.

2.2. Hardness measurements

The hardness of two types of butt-welded connections made of high strength steels S690, including VR690 joints that made between rolled steel S690 and rolled steel S690, CR690 joints that made between rolled steel S690 and cast steel G10MnMoV6-3 is experimentally investigated by Akyel [19].For S690, the yield strength and ultimate strength is 790 MPa and 847 MPa respectively, and the uniform elongation is 15%. For G10MnMoV6-3, the yield strength and ultimate strength 743 MPa and 799 MPa respectively, and the uniform elongation is 18.6%. The hardness measurements based on ISO-6507[20] were performed on the weld cross-section on the cap of the weld (CW), in the middle of the weld (MW), and at the root of the weld (RW) with an applied load of 9.807 N. The average value of all positions is denoted as AP. The hardness measurement locations are illustrated in Fig. 2. Noted that the width of the heat-affected zone is assumed to be 0.2 mm. The hardness distributions of VR690 joints and CR690 joints are shown in Figs. 3 and 4. The hardness value is largest at the heat affected zone while is smallest at the base materials for the cap of the weld and the middle of the weld, while the trend is not obvious for the root of the weld. The average value of hardness is listed in Tables 1 and 2. The results showed that the hardness value at the root of the welds is generally smaller than it at the cap of the weld and in the middle of the weld.

2.3. Fatigue life prediction using hardness values and hot-spot concept

The geometry of the butt-welded plate made of high strength steel is shown in Fig. 5-a, with a width of 160.0 mm, a length of 1000.0 mm, and a thickness of 25.0 mm. The plate width is reduced to 150 mm in the

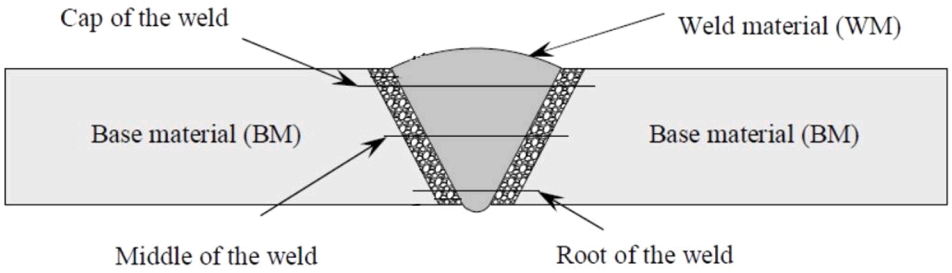

Fig. 2. Hardness measurement locations on a weld cross-section [19].

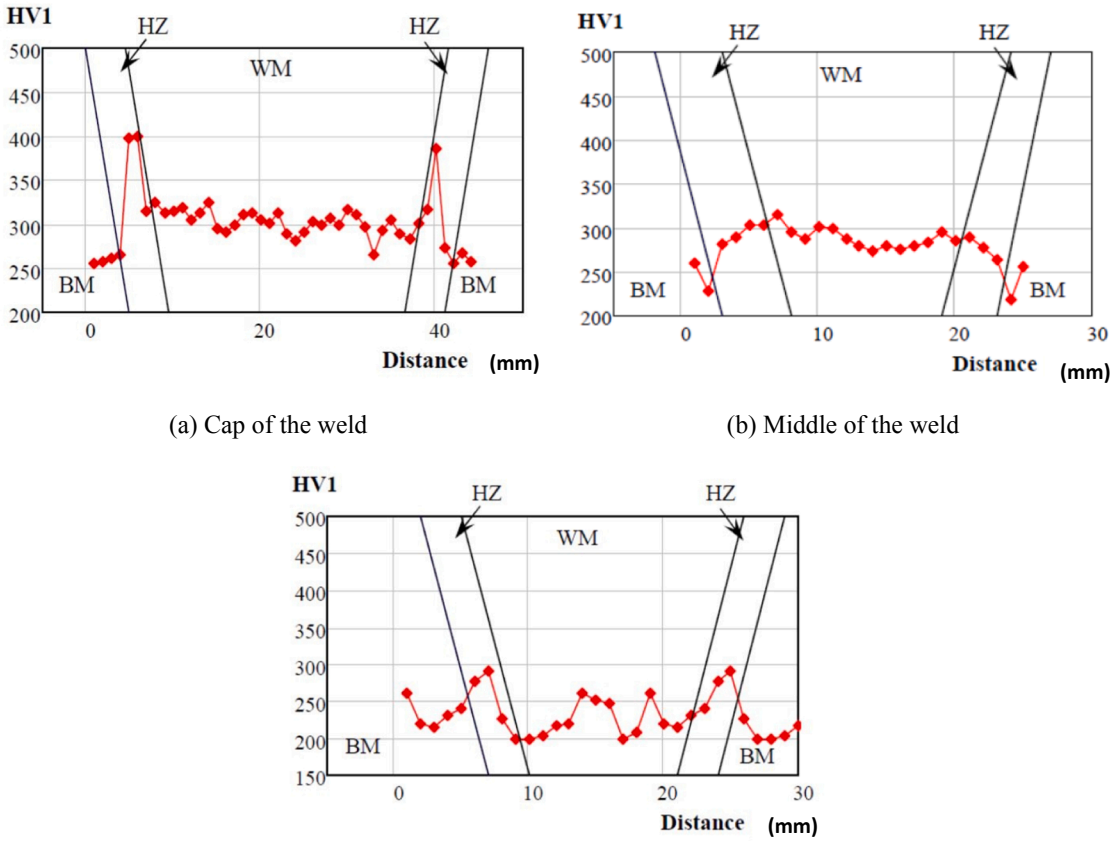

Fig. 3. Hardness distribution of VR690 joints [19].

middle of the specimen. Tests [19] of four types of butt-welded joints were conducted under cyclic loading at the Stevin II lab at the Delft University of Technology. The fatigue life, nominal strain range, and hot-spot stress range are summarized in Tables 3 and 4. The nominal strain range is measured through strain gauges shown in Fig. 5-b. The hot-spot stress of the critical position in Fig. 6 is calculated based on Eqs. (8) and (9) recommended by IIW [21]. The calculated hot-spot stresses, according to linear and quadratic extrapolations, respectively, obtained by Eqs. (8) and (9), are summarized in Tables 3 and 4 in terms of different welded joints. A discussion about the hot-spot stresses evaluation based on linear and quadratic extrapolation methods applied to finite element results and compared with experimental data for welded joints has been done by Lee et al. [22].

$$LE: \sigma_{hs} = 1.67\sigma_{0.4t} - 0.67\sigma_{1.0t} \tag{8}$$

$$\text{QE}: \sigma_{hs} = 2.52\sigma_{0.4t} - 2.24\sigma_{0.9t} + 0.72\sigma_{1.4t} \tag{9}$$

As shown in Fig. 7, fatigue cracks were initiated around the heat affected zone at the position "cap of welds" illustrated in Fig. 2. Hence, the hot-spot stress at different fatigue crack initiation life is calculated based on Eqs. (1)–(7) using the measured hardness at the position "cap of welds". The predicted hot-spot stresses based on linear and quadratic extrapolation methods are listed in Tables 5 and 6 for VR690 joints and Tables 7 and 8 for CR690 joints, respectively. A comparison between experimental results and the predicted fatigue life using the hardness value is shown in Fig. 8 for VR690 and Fig. 9 for CR690 joints, respectively. The results show that the predicted fatigue strength based on hardness is larger than from experimental observations. During the welding, the local heat introduces an abrupt temperature increase, followed by subsequent cooling to room temperature. A possible reason for the overestimated fatigue strength is lack of residual stress consideration (see Table 9).

Residual stress is calculated as the difference between predicted and experimental stresses. The predicted residual stress based on hardness

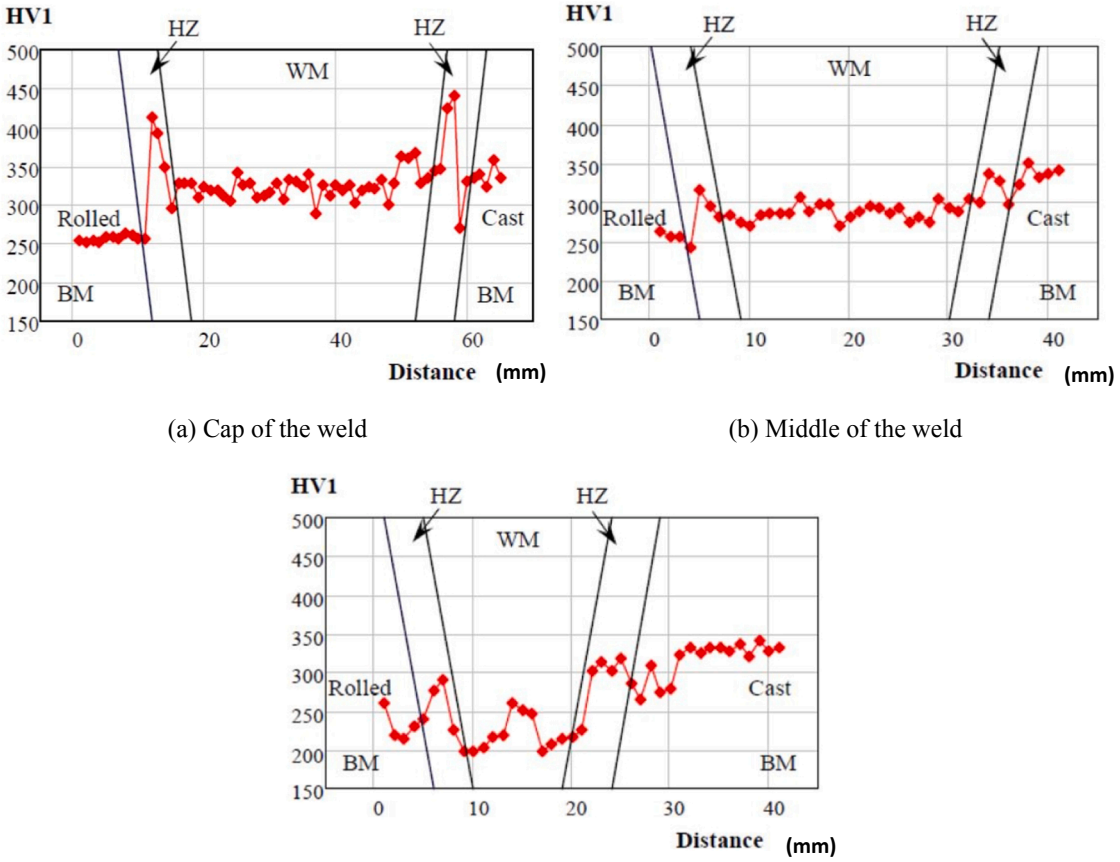

Fig. 4. Hardness distribution of CR690 joints [19].

Table 1
The hardness of VR690 (Unit: HV).

Positions	Welds		Heat Affected Zone (HAZ)		Base Materials (BM)	
	Ave.	Std.	Ave.	Std.	Ave.	Std.
Cap of the weld (CW)	301.85	13.56	323.09	57.91	258.96	5.56
Middle of the weld (MW)	289.22	11.29	287.50	12.63	241.42	20.18
Root of the weld (RW)	221.12	20.00	257.48	35.62	224.47	23.78
All Positions (AP)	283.63	14.13	292.29	48.89	235.55	24.42

Table 2
The hardness of CR690 (Unit: HV).

Positions	Welds		Heat Affected Zone (HAZ)		Base Materials (BM)	
	Ave.	Std.	Ave.	Std.	Ave.	Std.
Cap of the weld (CW)	324.39	15.98	346.20	60.71	282.54	41.04
Middle of the weld (MW)	287.59	9.98	298.97	29.23	307.62	40.66
Root of the weld (RW)	221.65	22.98	268.63	43.47	298.29	42.84
All Positions (AP)	298.42	15.98	307.75	54.88	294.44	41.80

using linear and quadratic extrapolation methods is summarized in Tables 5 and 6 for VR690 joints and Tables 7 and 8 for CR690 joints, respectively. For VR690 joints, the predicted residual stresses at the critical position using both linear and quadratic extrapolation is $0.33\sigma_y$ based on weld hardness, $0.39\sigma_y$based on hardness of the heat-affected zone (HAZ), and $0.23\sigma_y$ based on hardness of the base material. For CR690 joints, the predicted residual stress at the critical position using linear extrapolation is $0.35\sigma_y$ based on weld hardness, $0.40\sigma_y$ based on hardness of the heat-affected zone (HAZ), and $0.25\sigma_y$ based on hardness of the base material; using quadratic extrapolation, the predicted residual stress at the critical position is $0.34\sigma_y$ based on weld hardness, $0.40\sigma_y$ based on hardness of the heat-affected zone (HAZ), and $0.24\sigma_y$ based on hardness of the base material.

3. Residual stress prediction

In order to validate residual stresses based on hardness and test results, the welding process is numerically simulated to obtain the residual stress distribution. The details of the simulation are described in this section.

3.1. Material properties and welding procedures

The angle of the weld groove is 60° and the plates were welded by flux-cored arc welding (FCAW) using a ceramic backing plate. The macro graph of butt welds is shown in Fig. 10-a with the fusion and heat affected zone boundary marked with red lines. There are 23 welding layers for the butt welded joints [23]. The butt-welded joints were simplified as four passes to save the computational time, as shown in Fig. 10-b. Fig. 11 shows the temperature state for the assumed welding process, including the initial status, the spot welding, the first pass, the second pass, the third pass, the fourth pass, and the final state, cooling down to the room temperature same as the initial state.

Modelling of the welding procedure has been carried out using commercially available FEA software, ABAQUS [24]. A sequentially coupled thermo-mechanical analysis has been performed, where the

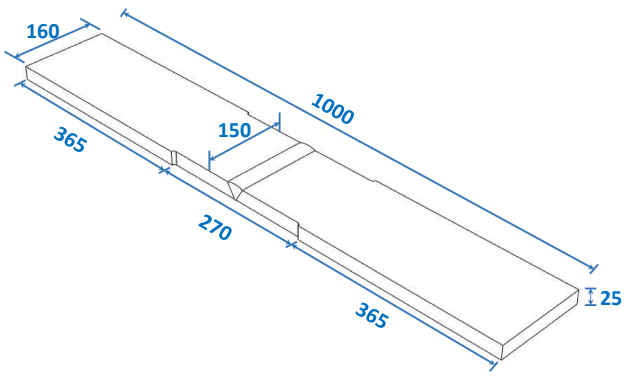

(a) Geometry

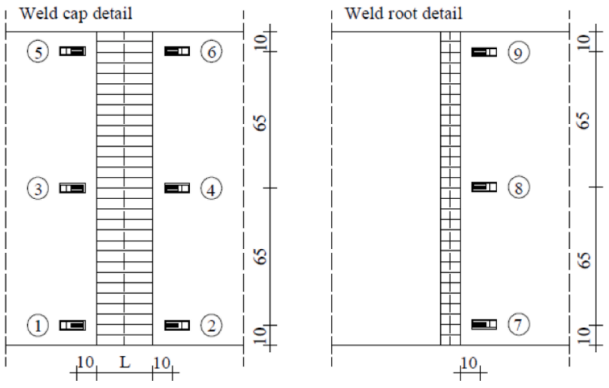

(b) Strain gauge layout [19]

Fig. 5. The geometry of butt welded plates (Unit: mm).

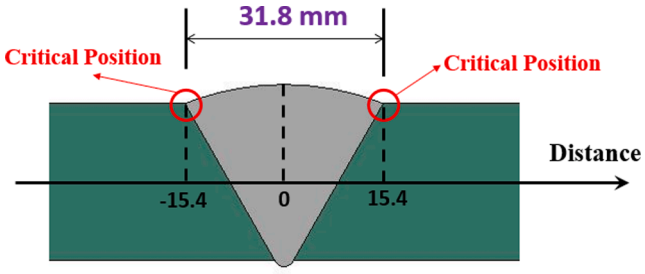

Fig. 6. Illustration of the critical positions.

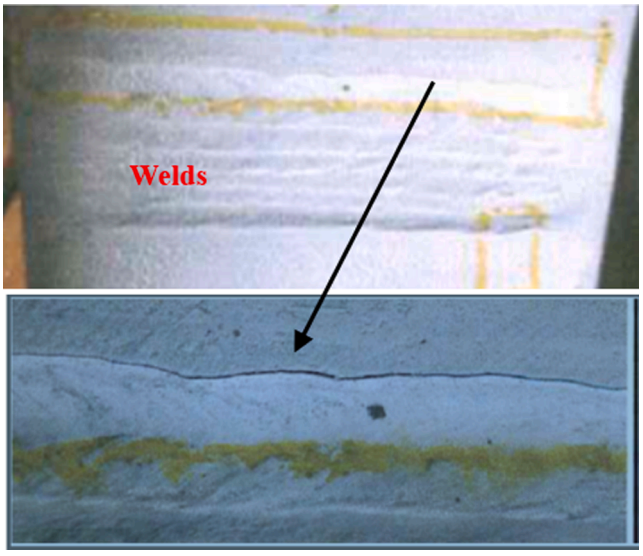

Fig. 7. Positions of initiated fatigue crack of butt-welded joints [19].

Table 3
Fatigue life summary of VR690 joints.

ID	Initiation Life	Failure Life	Nominal Strain Range ($\times 10^{-6}$)	Hot-spot stress by LE (MPa)	Hot-spot stress by QE (MPa)
1	378927	983687	967	204	208
2	208560	684565	1086	229	233
3	413035	644946	1052	222	226
4	166843	522021	1219	257	262
5	198636	551732	1205	254	259
6	337073	584540	1162	245	250
7	153723	362879	1224	258	263
8	186480	321962	1357	286	292
9	161106	243422	1476	311	317

Table 4
Fatigue life summary of CR690 joints.

ID	Initiation Life	Failure Life	Nominal Strain Amplitude ($\times 10^{-6}$)	Hot-spot stress by LE (MPa)	Hot-spot stress by QE (MPa)
1	–	4602408	967	204	208
2	393318	621920	1210	255	260
3	660161	1260937	1214	256	261
4	626931	854386	1057	223	227
5	890585	1141717	1081	228	232
6	534523	969052	1262	266	271
7	216127	367946	1443	304	310
8	166295	294947	1381	291	297
9	73537	149284	1529	322	329

Table 5
Predicted hot-spot stress based on linear extrapolation for VR690 joints using hardness at position "cap of welds".

Initiation Life	Hot-spot stress by LE (MPa)	Predicted Value (MPa)			Residual stress (MPa)		
		Welds	HAZ	BM	Welds	HAZ	BM
378927	204	474	511	403	270	307	199
208560	229	487	525	413	258	296	184
413035	222	472	509	401	250	287	179
166843	257	492	531	418	235	274	161
198636	254	488	526	414	234	272	160
337073	245	476	514	405	231	269	160
153723	258	494	533	419	236	275	161
186480	286	489	528	416	203	242	130
161106	311	493	532	419	182	221	108
Average					233.2	271.4	160.2

temperature field was introduced as a predefined field in the mechanical analysis. The stress–strain relationship of S690 steel is shown in Fig. 12 based on material tests at elevated temperature reported in ref. [25]. Additional thermal properties used in the FEA, shown in Fig. 13, are calculated based on the chemical composition in alloys of S690 steel as reported in ref. [26]. The annealing temperature is assumed as 1000 °*C* indicating that the plastic strains at the material points are setting to zero when the temperature is above it to consider the phase transition effect. The low end of the temperature range and the high end of temperature range within which the phase change occurs is assumed as 1450 °*C* and 1500 °*C*, respectively. The latent heat is assumed to be 247 J/g for consideration of released and absorbed thermal energy during the first-order phase transition.

Table 6
Predicted hot-spot stress based on quadratic extrapolation for VR690 joints using hardness at position "cap of welds".

Initiation Life	Hot-spot stress by QE (MPa)	Predicted Value (MPa)			Residual stress (MPa)		
		Welds	HAZ	BM	Welds	HAZ	BM
378927	208	474	511	403	266	303	195
208560	233	487	525	413	254	292	180
413035	226	472	509	401	246	283	175
166843	262	492	531	418	230	269	156
198636	259	488	526	414	229	267	155
337073	250	476	514	405	226	264	155
153723	263	494	533	419	231	270	156
186480	292	489	528	416	197	236	124
161106	317	493	532	419	176	215	102
Average					228.3	266.6	155.3

Table 7
Predicted hot-spot stress based on linear extrapolation for CR690 joints using hardness at position "cap of welds".

Initiation Life	Hot-spot stress by LE (MPa)	Predicted Value (MPa)			Residual stress (MPa)		
		Welds	HAZ	BM	Welds	HAZ	BM
–	204	469	504	404	265	300	200
393318	255	503	541	432	248	286	177
660161	256	489	526	421	233	270	165
626931	223	496	534	427	273	311	204
890585	228	491	528	423	263	300	195
534523	266	494	531	425	228	265	159
216127	304	514	553	442	210	249	138
166295	291	519	559	446	228	268	155
73537	322	536	578	460	214	256	138
Average					240.2	278.3	170.1

Table 8
Predicted hot-spot stress based on quadratic extrapolation for CR690 joints using hardness at position "cap of welds".

Initiation Life	Hot-spot stress by QE (MPa)	Predicted Value (MPa)			Residual stress (MPa)		
		Welds	HAZ	BM	Welds	HAZ	BM
–	208	469	504	404	261	296	196
393318	260	503	541	432	243	281	172
660161	261	489	526	421	228	265	160
626931	227	496	534	427	269	307	200
890585	232	491	528	423	259	296	191
534523	271	494	531	425	223	260	154
216127	310	514	553	442	204	243	132
166295	297	519	559	446	222	262	149
73537	329	536	578	460	207	249	131
Average					235.1	273.2	165.0

The boundary conditions for the butt-welded plate during mechanical analysis are presented in Fig. 14. The butt-welded plate is supported by four plates with two on the bottom and the other two on the top. The bottom surface of the bottom plates and the top surface of the top plates are fixed. General contacts were built between support plates and butt-welded plates with "hard" for normal direction and "penalty, friction coefficient 0.1" for tangential direction. Convection and radiation are considered by applying surface film contact with a coefficient of 15 W/(m^2 K) and surface radiation contact with emissivity, 0.9.

The welding torch is modelled with a heat boundary 1500 °C between the current welding fusion zone and the neighbouring zone. The current fusion elements are activated with a prescribed temperature of 1500 °C in the whole model after the welding torch passed the current fusion zone simulated by the steady heat transfer with defined pass time. Furthermore, additional fusion elements sets are created by the same nodes of welding elements used in the kill/birth simulation, and they are

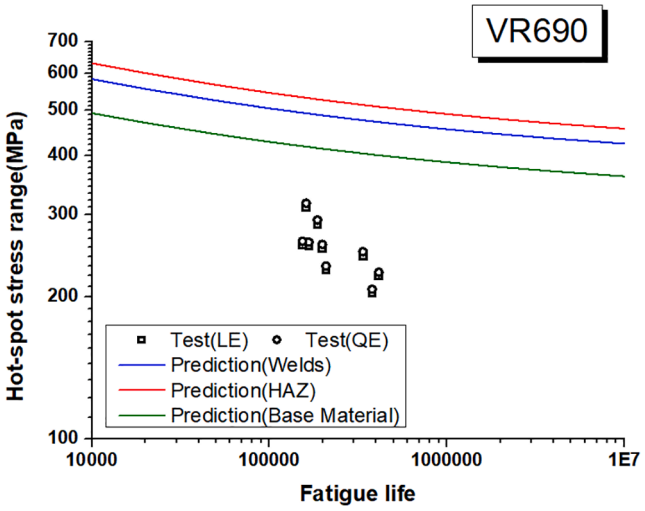

Fig. 8. Fatigue life comparison between predictions using different hardness measurements for VR690 joints.

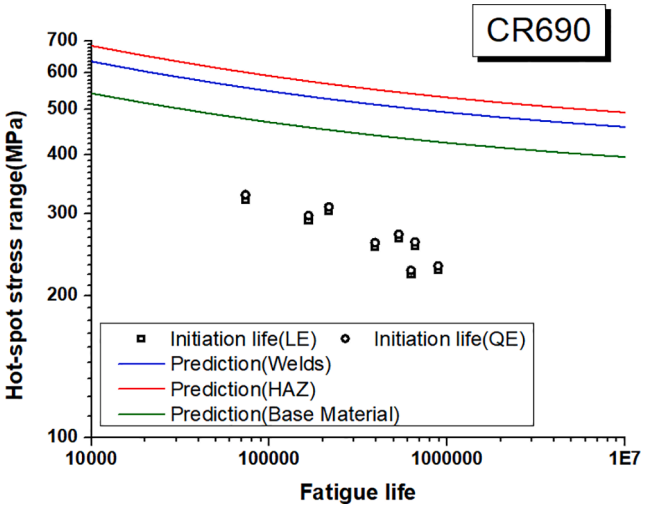

Fig. 9. Fatigue life comparison between predictions using different hardness measurements for CR690 joints.

assigned a very small elastic modulus during mechanical analysis. Two element types, weld elements and soft elements, exist at the same position on the welding fusion zone. The soft elements are excluded in the kill/birth simulation, and they deform with neglected resistance during mechanical analysis. Because the weld elements and soft elements share the same nodes, the positions of the weld elements also change due to the deformation of the soft elements.

3.2. Residual stress distribution

Fig. 15 shows the ratio of residual stress to yield stress along the welding direction based on FE analysis through-thickness at 5.0, 12.5, 20, and 35 mm from the centre of the welding line. Obtained results show that tensile residual stress along the welding direction is observed at 5.0, 12.5, 20 mm from the centre of the welding line, while compressive residual stress along the welding direction is found at 35 mm from the centre of the welding line. Park et al. [27] measured the welding residual stress of multi-pass butt-welded plates with a thickness of 25 mm and made of steel grade S460 using the neutron method. The FE residual stress pattern is validated here by comparing the FE results and those experimental results, and a satisfactory agreement is obtained.

Table 9
Comparisons between the average residual stress based on hardness and FE simulation.

		VR690			CR690		
		Positive Side	Negative Side	Average	Positive Side	Negative Side	Average
Welds	LE	14.70%	27.37%	21.04%	12.14%	25.19%	18.67%
	QE	16.49%	28.90%	22.70%	14.00%	26.78%	20.39%
HAZ	LE	0.73%	15.47%	8.10%	1.79%	13.32%	7.56%
	QE	0.07%	16.97%	8.52%	2.49%	14.91%	8.70%
BM	LE	41.40%	50.11%	45.76%	37.78%	47.02%	42.40%
	QE	43.20%	51.63%	47.42%	39.65%	48.61%	44.13%

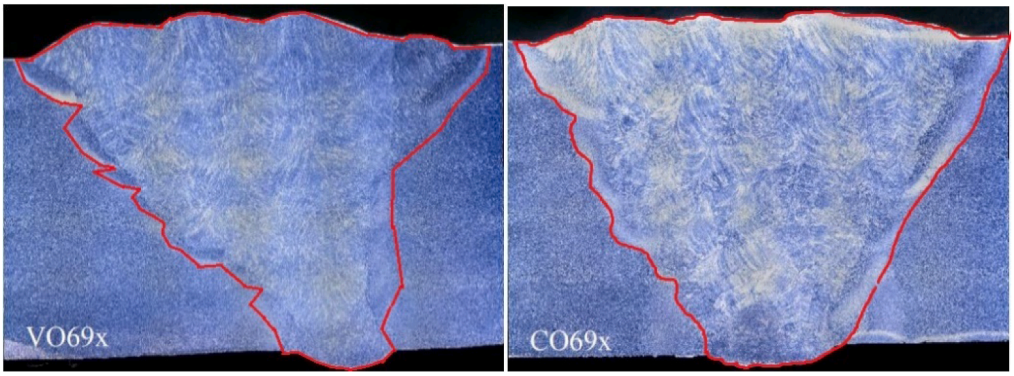

(a) Graph of butt welds [19]

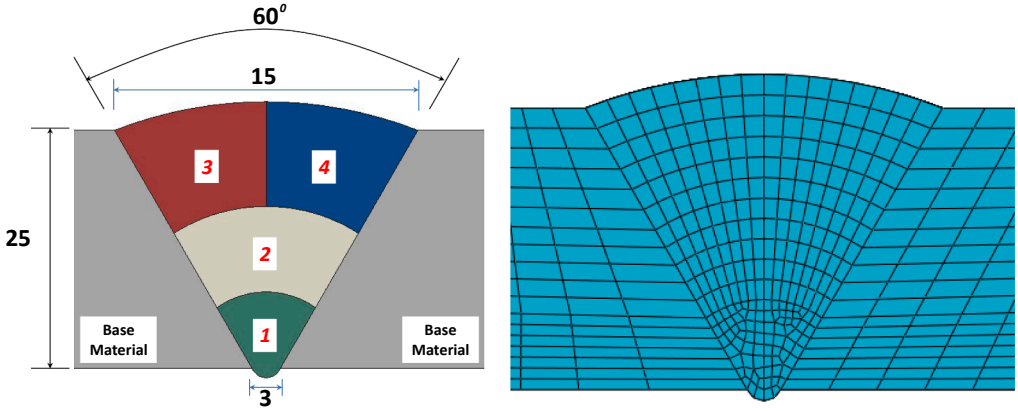

(b) Geometry and mesh of butt welds

Fig. 10. The geometry of butt-welded plates made of high strength steel (mm).

Note that a qualitative comparison of the stress distributions is considered since the steel grade was different in both cases. In the current study, 23 layers were simplified as four passes; the justification of these assumptions should be further investigated.

Fig. 16 shows the residual stress along the specimen length both in the welding direction and vertical to welding direction at t = 0, 12.5, and 25 mm in the thickness direction in the middle of the specimen. Based on Fig. 15-b, the residual stress along the transverse direction at the critical position (t = 25.0 mm) is determined to be 273.4 MPa when the distance from centre x = 15.4 mm, and is determined to be 321.08 MPa when the distance from centre x = −15.4 mm.

3.3. Residual stress comparisons

Comparisons between the average residual stress based on the measured hardness and FE simulation are quantified using Eq. (10) and summarized in Table 7. The average difference between the simulated residual stress and predicted residual stress using weld hardness is 21.04% and 22.70% for VR690 joints using LE and QE, respectively, and is 18.67% and 20.39% for CR690 joints using LE and QE, respectively. The average difference between the simulated residual stress and predicted residual stress using hardness of heat affected zone is 8.10% and 8.52% for VR690 joints using LE and QE, respectively, and is 7.56% and 8.70% for CR690 joints using LE and QE, respectively. The average difference between the simulated residual stress and predicted residual stress using hardness of the base material is 45.76% and 47.42% for VR690 joints using LE and QE, respectively, and is 42.40% and 44.13% for CR690 joints using LE and QE, respectively.

$$RME = \frac{\left|\Delta\sigma_{test,i} - \Delta\sigma_{predicted,i}\right|}{\Delta\sigma_{predicted,i}} \quad (10)$$

The results show that the residual stress predicted based on the hardness of the heat-affected zone (HAZ) agreed best with FE simulations among comparisons based on using the measured hardness of the weld, the heat-affected zone (HAZ), and the base material. This also agrees well with the failure modes where the fatigue crack is initiated

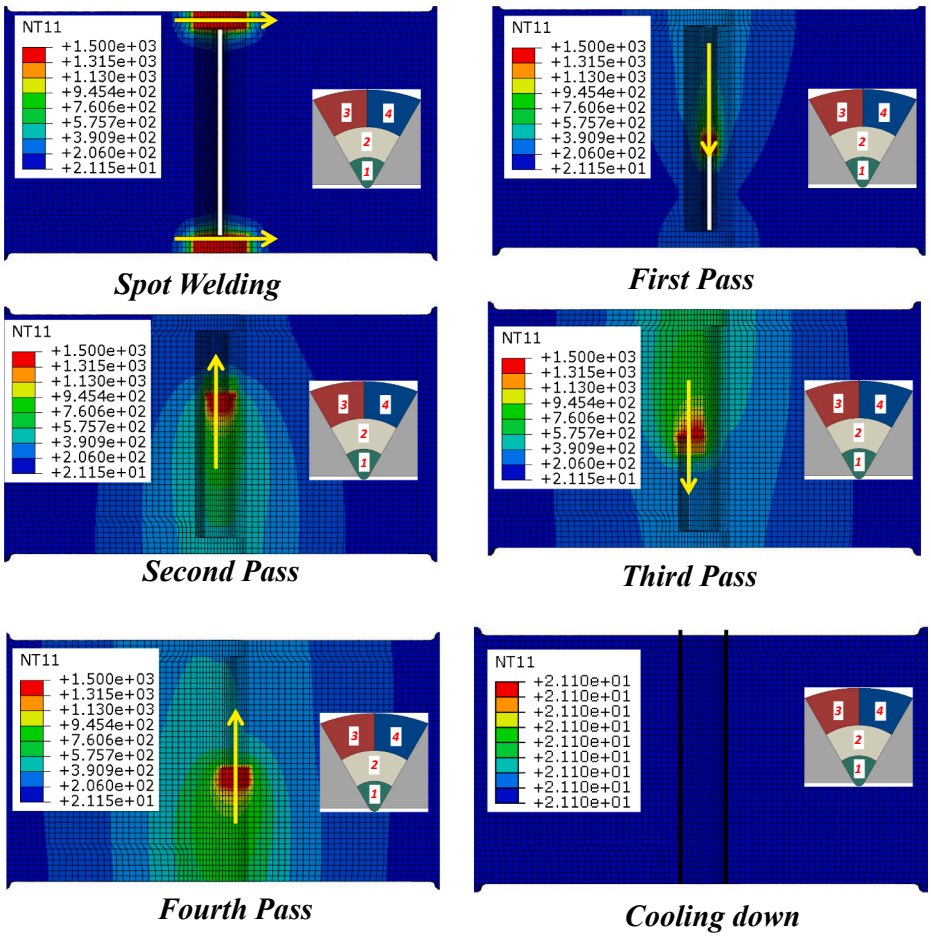

Fig. 11. Predicted temperature distribution during the welding process (Unit: °C).

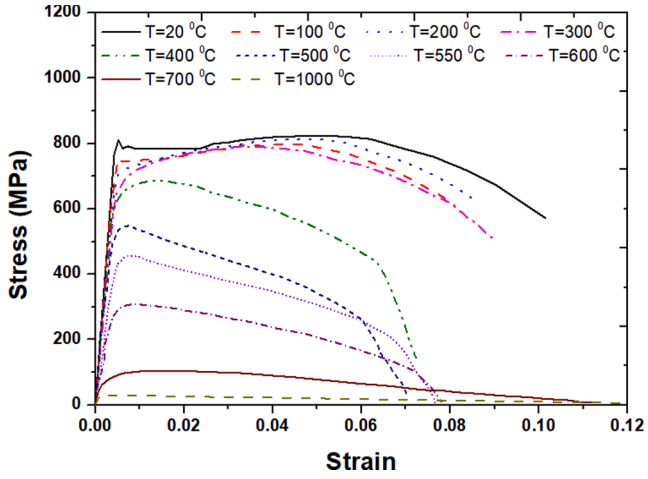

Fig. 12. Stress–strain relationship of S690 Steel [25].

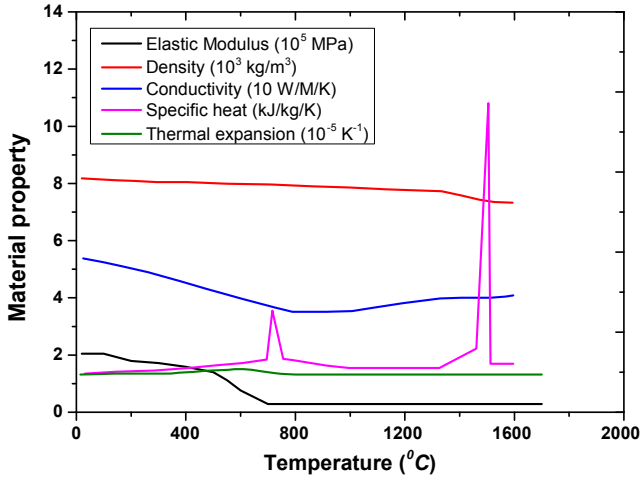

Fig. 13. Thermal and mechanical properties of S690 steel versus temperature [25,26].

near the heat-affected zone for the butt welded joints made of high strength steel S690. Besides, the simulated residual stress at the positive distance side agrees better with the hardness predicted residual stress than the corresponding simulated residual stress at the negative distance side.

The differences in predicted residual stress between LE and QE are quite small. The predicted residual stress based on LE is used to improve fatigue life prediction, as shown in Figs. 17 and 18. After considering the residual stress, the predicted S-N curve agrees better with the test results.

4. Conclusions

One of the most challenging issues is how to predict the fatigue life of welded structures with complex geometry based on test results from relatively simple coupon specimens. Difficulties in predicting welded structural steel fatigue behaviour based on results at the coupon level

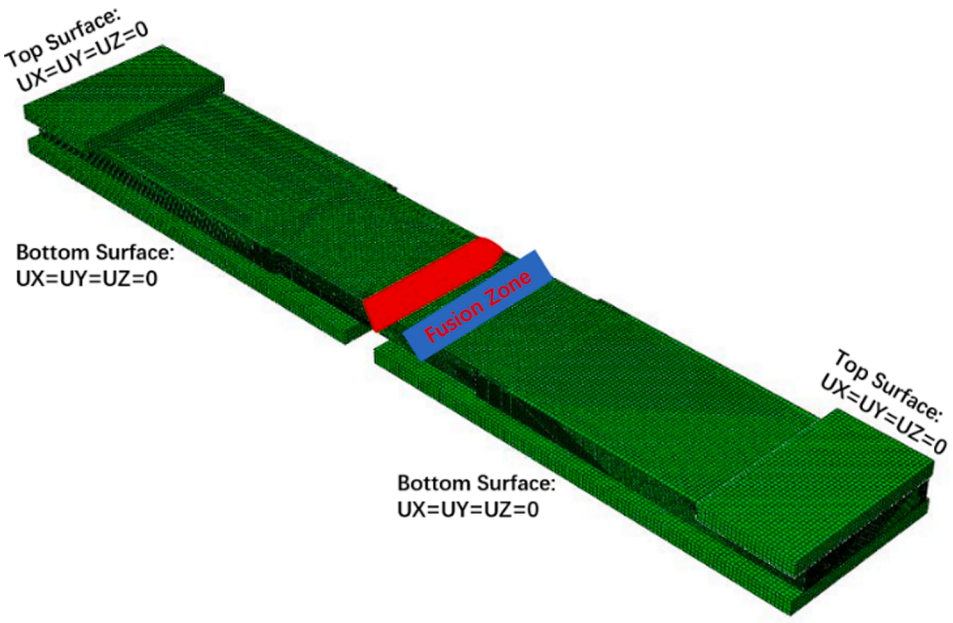

Fig. 14. Boundary conditions for mechanical analysis.

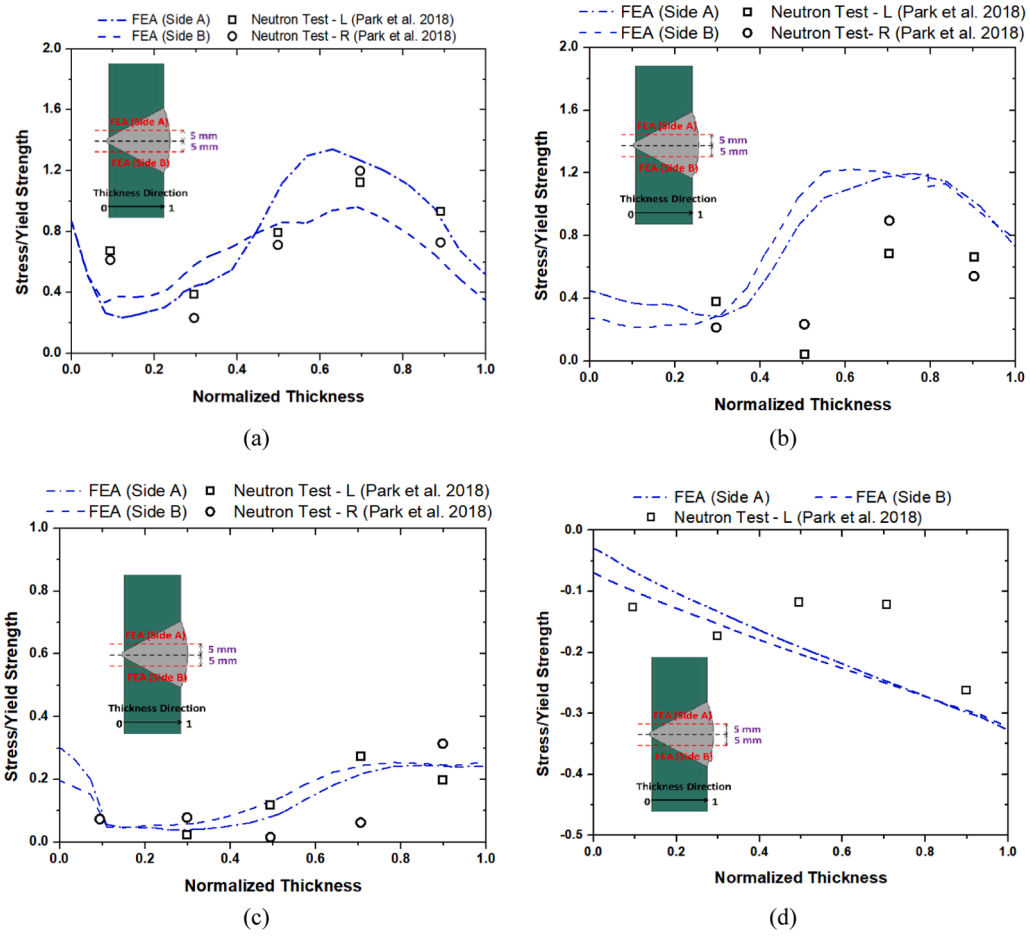

Fig. 15. Comparisons between FE analyses and experimental results [27].

are greater in the presence of pre-existing residual stresses in the welded coupon specimens as residual stresses vary a lot in welded structures with complex geometry. In this paper, a residual stress-free property, hardness, is employed to predict the fatigue life of butt-welded joints.

The following conclusions may be drawn from this study:

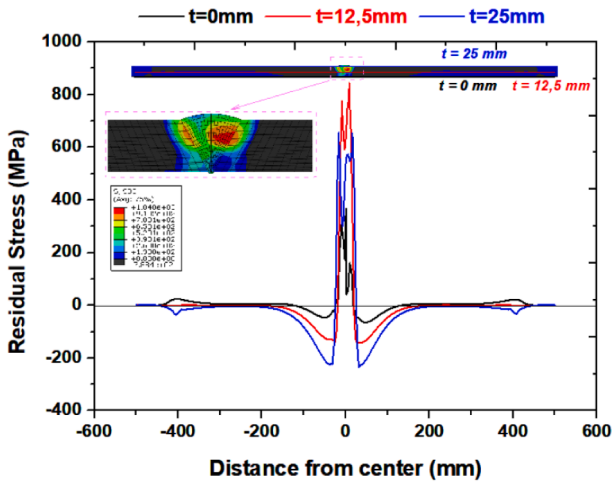

(a) Welding direction

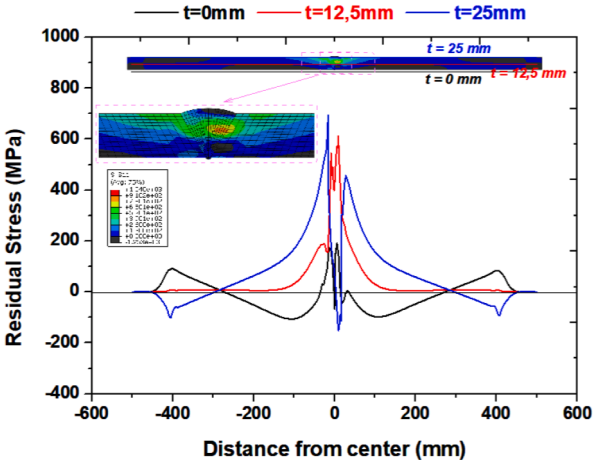

(b) Transverse direction

Fig. 16. Residual stress distribution along the specimen length.

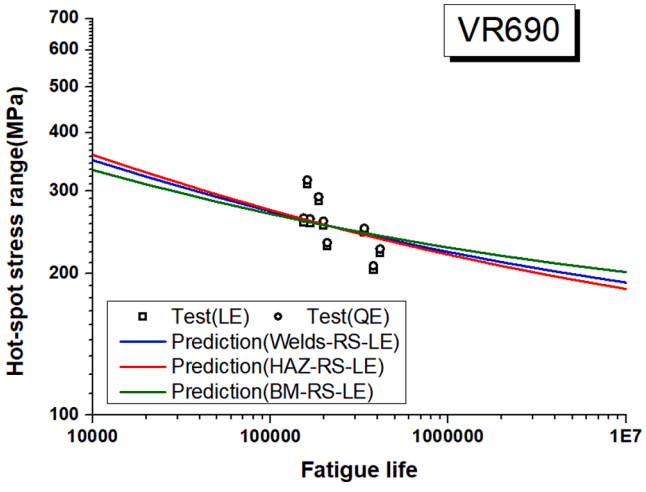

Fig. 17. Fatigue life comparison between prediction using hardness measurements considering residual stress effects and experimental observations for VR690 joints.

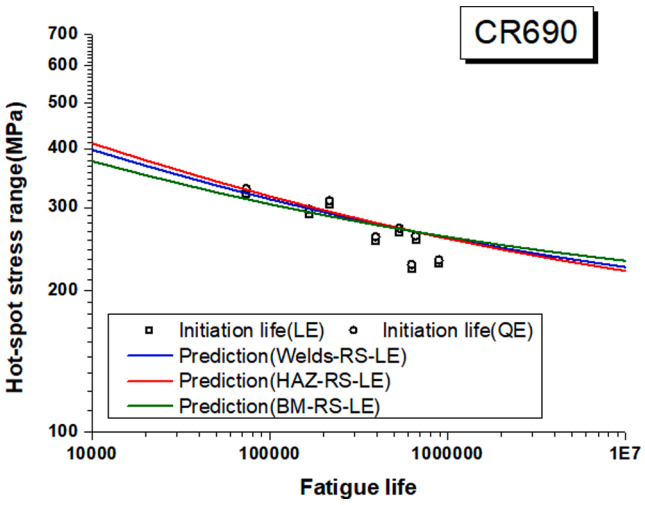

Fig. 18. Fatigue life comparison between prediction using hardness measurements considering residual stress effects and experimental observations for CR690 joints.

(1) The full range of S-N curves based on hardness measurements without considering residual stress effects overestimates fatigue life of butt-welded joints.
(2) The experimental fatigue data of butt-welded joints made of high strength steels based on hardness measurements and using the hot-spot concept seem to be useful to estimate residual stress effects.
(3) Residual stress is calculated as the difference between predicted and experimental stresses. The predicted residual stress at the root of the welds is 0.24–0.39σ_y for VR690 joints using hardness at different positions, and the predicted residual stress at the root of the welds is 0.25–0.40σ_y for CR690 using hardness at different positions.
(4) The residual stress predicted based on hardness of the heat-affected zone (HAZ) agrees best with FE simulations with a maximum error of 8.52% for VR690 joints and 8.70% for CR690 joints, for failure modes where the fatigue crack is initiated near the heat-affected zone for the butt welded joints made of high strength steel S690. Besides, the simulated residual stress at the positive distance side agreed better with hardness predicted residual stress than the simulated residual stress at the negative distance side. After considering residual stresses, the predicted S-N curve agrees better with test results than they do when residual stresses are not considered.

CRediT authorship contribution statement

Haohui Xin: Investigation, data analysis, writing. **José A.F.O. Correia:** Writing and validation. **Milan Veljkovic:** Writing and review. **Filippo Berto:** Writing and review. **Lance Manuel:** Writing and review.

Declaration of Competing Interest

The authors declare that they have no known competing financial interests or personal relationships that could have appeared to influence the work reported in this paper.

Acknowledgments

This research was supported by the National Natural Science Foundation (Grants #51808398) of the People's Republic of China, project grant (UTA-EXPL/IET/0111/2019) SOS-WindEnergy - Sustainable Reuse of Decommissioned Offshore Jacket Platforms for Offshore Wind

Energy by national funds (PIDDAC) through the Portuguese Science Foundation (FCT/MCTES); and, base funding - UIDB/04708/2020 and programmatic funding - UIDP/04708/2020 of the CONSTRUCT - Instituto de I&D em Estruturas e Construções - funded by national funds through the FCT/MCTES (PIDDAC). The authors would also like to thank all support by UT Austin Portugal Programme.

References

[1] Veljkovic M, Johansson B. Design of hybrid steel girders. J Constr Steel Res 2004; 60:535–47.
[2] Xin H, Veljkovic M. Fatigue crack initiation prediction using phantom nodes-based extended finite element method for S355 and S690 steel grades. Eng Fract Mech 2019;214:164–76.
[3] Xin H, Correia JAFO, Veljković M. three-dimensional fatigue crack propagation simulation using extended finite element methods for steel grades S355 and S690 considering mean stress effects. Eng Struct 2020;227:111414.
[4] Macdonald K. Fracture and fatigue of welded joints and structures. Elsevier; 2011.
[5] Rozumek D, Lewandowski J, Lesiuk G, Correia JA. The influence of heat treatment on the behavior of fatigue crack growth in welded joints made of S355 under bending loading. Int J Fatigue 2020;131:105328.
[6] Burk J, Lawrence F. The effect of residual stresses of weld fatigue life. 1978.
[7] Xin H, Veljkovic M. Residual stress effects on fatigue crack growth rate of mild steel S355 exposed to air and seawater environments. Mater Des 2020;108732.
[8] Xin H, Veljković M. Effects of residual stresses on fatigue crack initiation of butt-welded plates made of high strength steel. Seventh Int. Conf. Struct. Eng. Mech. Comput., Cape Town/South Africa: 2019, p. 1260–6.
[9] Teng TL, Fung CP, Chang PH. Effect of weld geometry and residual stresses on fatigue in butt-welded joints. Int J Press Vessel Pip 2002;79:467–82. https://doi.org/10.1016/S0308-0161(02)00060-1.
[10] Teng TL, Chang PH. Effect of residual stresses on fatigue crack initiation life for butt-welded joints. J Mater Process Technol 2004;145:325–35. https://doi.org/10.1016/j.jmatprotec.2003.07.012.
[11] Dong Y, Garbatov Y, Guedes Soares C. Fatigue crack initiation assessment of welded joints accounting for residual stress. Fatigue Fract Eng Mater Struct 2018; 41:1823–37. https://doi.org/10.1111/ffe.12824.
[12] Bandara CS, Siriwardane SC, Dissanayake UI, Dissanayake R. Developing a full range S-N curve and estimating cumulative fatigue damage of steel elements. Comput Mater Sci 2015;96:96–101.
[13] Bandara CS, Siriwardane SC, Dissanayake UI, Dissanayake R. Full range S-N curves for fatigue life evaluation of steels using hardness measurements. Int J Fatigue 2016;82:325–31.
[14] Strzelecki P, Tomaszewski T. Analytical models of the S-N curve based on the hardness of the material. Procedia Struct Integr 2017;5:832–9.
[15] Correia JAFO, et al. A generalization of the fatigue Kohout-Věchet model for several fatigue damage parameters. Eng Fract Mech 2017;185.
[16] Roessle ML, Fatemi A. Strain-controlled fatigue properties of steels and some simple approximations. Int J Fatigue 2000;22:495–511.
[17] Shamsaei N, Fatemi A. Effect of hardness on multiaxial fatigue behaviour and some simple approximations for steels. Fatigue Fract Eng Mater Struct 2009;32:631–46.
[18] Frankel J, Abbate A, Scholz W. The effect of residual stresses on hardness measurements. Exp Mech 1993;33:164–8.
[19] Akyel A. Fatigue strength of repaired cracks in welded connections made of very high strength steels. Delft University of Technology; 2017.
[20] Standard EN. ISO 6507-1: 2007. Metallic materials. Vickers hardness test. Test Method n.d.
[21] Hobbacher A. Recommendations for fatigue design of welded joints and components. Springer; 2016.
[22] Lee, J.-., Seo, J.-., Kim, M.-., Shin, S.-., Han, M.-., Park, J.-. & Mahendran M. Comparison of hot spot stress evaluation methods for welded structures. Int J Nav Archit Ocean Eng 2010;2:200–10.
[23] Pijpers RJM. Fatigue strength of welded connections made of very high strength cast and rolled steels. 2011.
[24] Abaqus V. 6.14 Documentation. Dassault Syst Simulia Corp 2014.
[25] Qiang X, Bijlaard F, Kolstein H. Dependence of mechanical properties of high strength steel S690 on elevated temperatures. Constr Build Mater 2012;30:73–9. https://doi.org/10.1016/j.conbuildmat.2011.12.018.
[26] Gao H. Residual stress development dur to high-frequency post weld impact treatments for high-strength steels. Delft University of Technology; 2014.
[27] Park J ung, An G, Woo W. The effect of initial stress induced during the steel manufacturing process on the welding residual stress in multi-pass butt welding. Int J Nav Archit Ocean Eng 2018;10:129–40. Doi: 10.1016/j.ijnaoe.2017.02.007.